ISSN 0016-7932, Geomagnetism and Aeronomy, 2017, Vol. 57, No. 4, pp. 491–499. © Pleiades Publishing, Ltd., 2017.
Original Russian Text © V.V. Bychkov, L.P. Korsunova, S.E. Smirnov, V.V. Hegai, 2017, published in Geomagnetizm i Aeronomiya, 2017, Vol. 57, No. 4, pp. 532–540.

Atmospheric Anomalies and Anomalies of Electricity in the Near-Surface Atmosphere before the Kamchatka Earthquake of January 30, 2016, Based on the Data from the Paratunka Observatory

V. V. Bychkov[a, *], L. P. Korsunova[b, **], S. E. Smirnov[a, *], and V. V. Hegai[b, ****]**

[a] *Institute of Space Physics Research and Propagation of Radio Waves, Far East Branch of the Russian Academy of Sciences, Paratunka village, Yelizovo district, Kamchatka Krai, Russia*

[b] *Pushkov Institute of Terrestrial Magnetism, Ionosphere, and Propagation of Radio Waves, Russian Academy of Sciences, Troitsk, Moscow oblast, Russia*

**e-mail: vasily.v.bychkov@gmail.com*

***e-mail: lpkors@rambler.ru*

****e-mail: sergey.ed.smirnov@gmail.com*

*****e-mail: hegai@izmiran.ru*

Received May 19, 2016; in final form, October 13, 2016

Abstract—The 15-min data of vertical ionosphere sounding and 10-min data from measurements of the vertical component (*Ez*) of the near-surface quasistatic atmospheric electrical field and the respective values of electrical conductance of near-surface air at the Paratunka complex geophysical observatory in the period from January 28 to January 30, 2016 have been analyzed to reveal the possible anomalies preceding the $M = 7.2$ earthquake that occurred on January 30, 2016, at 0325 UT. The distance between the observatory and epicenter was 117 km. These anomalies have been revealed, and the majority of them, in our opinion, may be related to the processes of earthquake preparation.

DOI: 10.1134/S0016793217040053

1. INTRODUCTION

The analysis of various experimental data obtained in the preparation zone of a strong earthquake shortly before the mainshock is always of great interest. Such an analysis is necessary, first, to obtain the fullest physical understanding of the subsequent seismic event and, in the future, to determine the specific features that appear at the final stage of earthquake preparation.

The ultimate goal of all of these studies is to determine the set of precursory anomalies in the behavior of various measured physical parameters that would serve as possible time indicators of the upcoming quake (its possible precursors) to be used in predictions of earthquakes. However, the identification of earthquake precursory anomalies (EPAs) in a given preceding time period does not necessarily indicate an unavoidable link between the anomalies and earthquakes, even in the case of a stable correlation with a particular characteristic warning time (for example, dependence on earthquake magnitude). In any case, observational data must be collected to address both fundamental questions about the possible cause-and-effect relationships between EPAs and subsequent earthquakes and to solve practical problems of earthquake prediction if some set of EPAs were to show a strong correlation to the moment of earthquake occurrence and take place within the desired preceding time.

The present work does not discuss the genesis of seismogenic anomalies that manifest in the atmosphere before earthquakes and are caused by earthquake preparation processes within regions of their sources in the Earth's interior. The possible physical mechanisms of relationships between earthquake-preceding ionospheric disturbances (EPIDs), which can be considered ionospheric precursors of earthquakes (IPEs), are considered in detail, in particular, in the monographs by Liperovskii et al. (1992) and Pulinets and Boyarchuk (2004), while earthquake precursory anomalies in near-surface atmospheric electricity (EPANAE) that are electrical earthquake precursors (EEPs) have been comprehensively considered in a monograph (*Elektromagnitnye* ..., 1982) and also in publications (Rulenko, 2000, 2008). An important physical aspect of the direct relationship between seismogenic electrical anomalies in the solid earth before earthquakes and their respective manifestations in the near-surface atmosphere due to the transfer of positively charged “holes” (which occurs with compression in igneous rocks) has been comprehensively described by St-Laurent et al. (2006) and Freund et al. (2006). A general overview of all possible types of earthquake precursors and their physical natures have been discussed in detail in the monograph by A.Ya. Sidorin (1992).

The goal of the present work is to distinguish IDPEs and EPANAEs, as well as to perform a comparative analysis of their behavior before the Kamchatka earthquake (the geographic coordinates of the epicenter are $\varphi_e = 54.01°$ N and $\lambda_e = 158.01°$ E, magnitude is $M = 7.2$, hypocentral depth is $h = 161$ km) of January 30, 2016, that occurred at 0325 UT at the epicentral distance of $R \cong 117$ km from the Paratunka complex geophysical observatory (the geographic coordinates are $\varphi = 52.97°$ N, $\lambda = 158.25°$ E). For this purpose, we used the measurements of ionospheric parameters (15-min sampling frequency) and measurements of the the vertical component (*Ez*) of near-surface quasistatic atmospheric electrical field (QAEF) with the respective values of electrical conductivity of near-surface air (λ^+ and λ^-) measured every 10 min in January 2016.

Here, we should note that the considered earthquake belongs to the class of intermediate hypocentral depth ($60 \leq h \leq 300$ km). Since the epicentral zone of an earthquake is usually determined as a projection of a source zone to the Earth’s surface, with the most intensive macroseismic effects being manifested within this zone, the extent of earthquake preparation zone on the Earth’s surface is at least comparable to that of the epicentral zone.

According to the data from the United States Geological Survey (USGS), the characteristic size of epicentral zone for this earthquake is ~1000 km, while the Paratunka Observatory, which is located 117 km from the epicenter and is very close to the center of earthquake preparation zone on the Earth’s surface. Moreover, it appears (Aprodov, 2000) that the deeper earthquake source is, the larger is the area covered by seismic manifestation at the same earthquake energy—i.e., manifestations of earthquakes with intermediate depths (the hypocenters are at depths of 60 to 300 km) cover larger areas as compared to earthquakes with hypocenters located in the crust (down to a depth of 60 km) at the same magnitudes. In addition, if to take into consideration possible manifestations of anomalies in the ionosphere before this earthquake, we must remember that G.T. Nestorov in his pioneering work (1979) identified seismoionospheric disturbances in the ionosphere 2 h before the strong Vrancea earthquake of March 4, 1977, from observations along radio paths running immediately above the epicentral zone of this earthquake. The discussed earthquake had magnitude $M = 7.2$ and its hypocentral depth was 120 km, so this event was also of intermediate depth.

2. GEOPHYSICAL AND METEOROLOGICAL SETTINGS

In analyzing the ionospheric variations, a considerable role is played by either the presence or absence of significant geomagnetic disturbances in the considered time period, because these disturbances can affect the entire ionosphere (their global effect on the ionosphere *F* region is particularly strong (Rishbeth, 1991; Prölss, 1995)); additionally, studies of near-surface electricity can be complicated by the presence of precipitation (Mikhailov et al., 2005; Rulenko, 2008).

Below, we will consider in detail the behavior of ionospheric parameters and characteristics of near-surface atmospheric electricity during the 3-day interval from January 28 until January 30, 2016 (i.e., the period including two days before the earthquake and the day it occurred). In order to distinguish the disturbances of studied parameters, we should know their background levels. In this respect, to obtain the background (reference) level of the respective reference median values for the considered parameters, we chose broader time intervals. In particular, in the case of near-surface atmospheric electricity, this interval was 7 days (January 25 to January 30, 2016), while we added the day of February 2, 2016 (thus, eight days on aggregate), in the case of calculating median values of ionospheric characteristics. This choice was made for the following reasons.

First, there was no precipitation from January 25 to January 31 UT, according to the data from Paratunka Observatory. The noise level in the QAEF signal in the presence of precipitation is two orders higher as compared to the “clear sky” condition—this could complicate the identification of anomalies (Mikhailov et al., 2005).

Second, according to the World Data Center for Geomagnetism, Kyoto, Japan (http://wdc.kugi.kyoto-u.ac.jp/index.html), the value of *Kp*-index of planetary geomagnetic activity sampled every 3 h did not exceed 2_+ (this corresponds to quiet geomagnetic conditions) during the entire period under consideration, except for the last 3 h of January 31.

In order to increase the length of sampling of ionospheric data up to that of the data on near-surface atmospheric electricity, we additionally considered the day of February 2, 2016, which was quiet in the geomagnetic sense; this day was chosen because the representativeness of ionospheric data on January 31 was small (only the first 3 h and last 3 h were available). The day of February 1, 2016, was not included in the sampling, because there were values of *Kp*-index 3_- and 4_-, respectively, in the interval 0000–0006 UT (i.e., the geomagnetic state exceeded the quiet level for 6 h).

3. METHOD OF DATA PROCESSING

Data processing was made in a uniform manner (in the cases of both absolute and relative measurements) for all of the time series of physical parameters considered in the present work, by a technique close to that described by Korsunova and Hegai (2008) and Korsunova and Hegai (2014).

The procedure included the following. First, the median value $Y_{med}(t_i)$ was calculated for the desired physical parameter $Y(t_i)$ on the chosen set of days and for each moment of time during a day (the sampling frequency was 15 min for ionospheric characteristics and 10 min for the electrical parameters of the near-surface atmosphere). We then analyzed the desired absolute or relative differences between the current and median values of considered parameters bound to the respective time count t_i on a daytime interval $[\Delta Y(t_i) = Y_{current}(t_i) - Y_{med}(t_i)$ and $\Delta Y(t_i)/Y_{med}(t_i)]$ during the 3-day period of January 28 to January 30, 2016 (see section 2 above).

We chose the interquartile range *IQR* (the difference between the upper and lower quartiles of the respective parameter) as calculated on the mentioned 3-day interval to be the measure of random deviation scatter. In this case, "noise" bands $K\pm = [\Delta Y(t_i)]_{\mathrm{MED}} \pm 1.5IQR$ or $K\pm = [\Delta Y(t_i)/Y_{med}(t_i)]_{\mathrm{MED}} \pm 1.5IQR$ would confine the possible variations in parameters explained by random deviations with some degree of probability. According to the *Encyclopedia of Statistical Sciences* (Klotz and Johnson, 1983), in the case of the normal distribution of "error" in values of $\Delta Y(t_i)$ (or $\Delta Y(t_i)/Y_{med}(t_i)$), the value $1.5IQR$ would correspond to approximately double standard deviations. Under the effect of various random factors, the value $\Delta Y(t_i)$ (or $\Delta Y(t_i)/Y_{med}(t_i)$) should vary within the limits of the mentioned noise bands $K\pm$ with a probability of 95%, or, putting it another way, the probability that values went beyond $K\pm$ band because of some random factors is as small as 5%. We considered values $\Delta Y(t_i)$ and $\Delta Y(t_i)/Y_{med}(t_i)$ beyond the limits of mentioned noise bands to be anomalous values $Y_{current}(t_i)$ if the duration of such disturbance was at least half an hour, because they are not random with a probability 95%.

Here we should note that a successful identification of seismoionospheric anomalies in the behavior of the critical frequency of the ionosphere $F2$-region on the basis of *IQR* as a measure of deviation from the background has been done earlier (Liu et al., 2006)—the only difference was that these authors used the value $IQR/2$ as the initial measure of deviation from the background. Thus, we use a more rigid criterion to select the deviated values that can be referred to disturbed values of considered parameters.

The efficiency of the method applied in this work for the discovery of seismoionospheric anomalies in the epignosis from solely ionospheric data was estimated earlier by Korsunova and Hegai (2013), in accordance with one of the algorithms described by Chen et al. (2004).

This implies the compilation of a contingency table for the selected observation interval. The days are arranged on a 2 × 2 matrix in accordance with their characteristics, and Hansen–Kuipers estimate (Hanssen-Kuipers Score, True Skill Statistic, Pierce Skill Score, Rscore) (Chen et al., 2004) is then used. It is the difference between the probability of revealing a true seismoionospheric anomaly, i.e., one preceding an earthquake within a given time period (in (Korsunova and Hegai, 2013), the preceding interval was determined to be ≤3 days), and the probability of a false alarm." Numerically, this estimate can range from –1 to 1, and the latter value means a 100% probability of revealing a true seismoionospheric anomaly with the absence of "false alarms. In the case of processed series of earthquakes in the Kamchatka region, in the magnitude range $M = 4.6–6.0$, the *Rscore* value obtained by Korsunova and Hegai (2013) was 0.82, which is quite high. It must be emphasized that the case analyzed below of the discussed earthquake is similar to the seismoionospheric anomalies distinguished earlier by the same method and in the same region but for weaker earthquakes and from ionospheric data only (Korsunova and Hegai, 2013, 2014, 2015). In contrast to these works, we involved independent measurements of electrical characteristics of the near-surface atmosphere.

In our work, we will consider the temporal variations of the following physical parameters:

—*h'Es*, the smallest virtual height of the sporadic *E* region for an ordinary wave;

—*foEs*, the limit frequency of an ordinary wave of the ionosphere sporadic *E* region;

—*fbEs*, the screening frequency of an ordinary wave of the ionosphere sporadic *E* region;

—*foF*2, the critical frequency of an ordinary wave of the ionosphere *F*2 region;

—γ, the factor of unipolarity in the near-surface atmosphere, is determined as the ratio between the absolute value of specific electrical conductivity of near-surface air, which is caused by positive ions, $\mathrm{abs}(\lambda^+)$, to the absolute value of specific electrical conductivity of near-surface air, which is caused by negative ions, $\mathrm{abs}(\lambda^-)$;

—*Ez*, the vertical component of near-surface QAEF; and

—*Jz*, the density of vertical conductivity current in near-surface air layer, which is determined as product of $\lambda_\Sigma Ez$, where $\lambda_\Sigma = \mathrm{abs}(\lambda^+) + \mathrm{abs}(\lambda^-)$.

4. RESULTS AND DISCUSSION

Figure 1 presents the variations in the chosen (see section 3) ionospheric parameters during the 3-day period (UT). The dashed line with arrow marks the moment of earthquake occurrence; the dark rectangles on the abscissa axis show the intervals from 1800

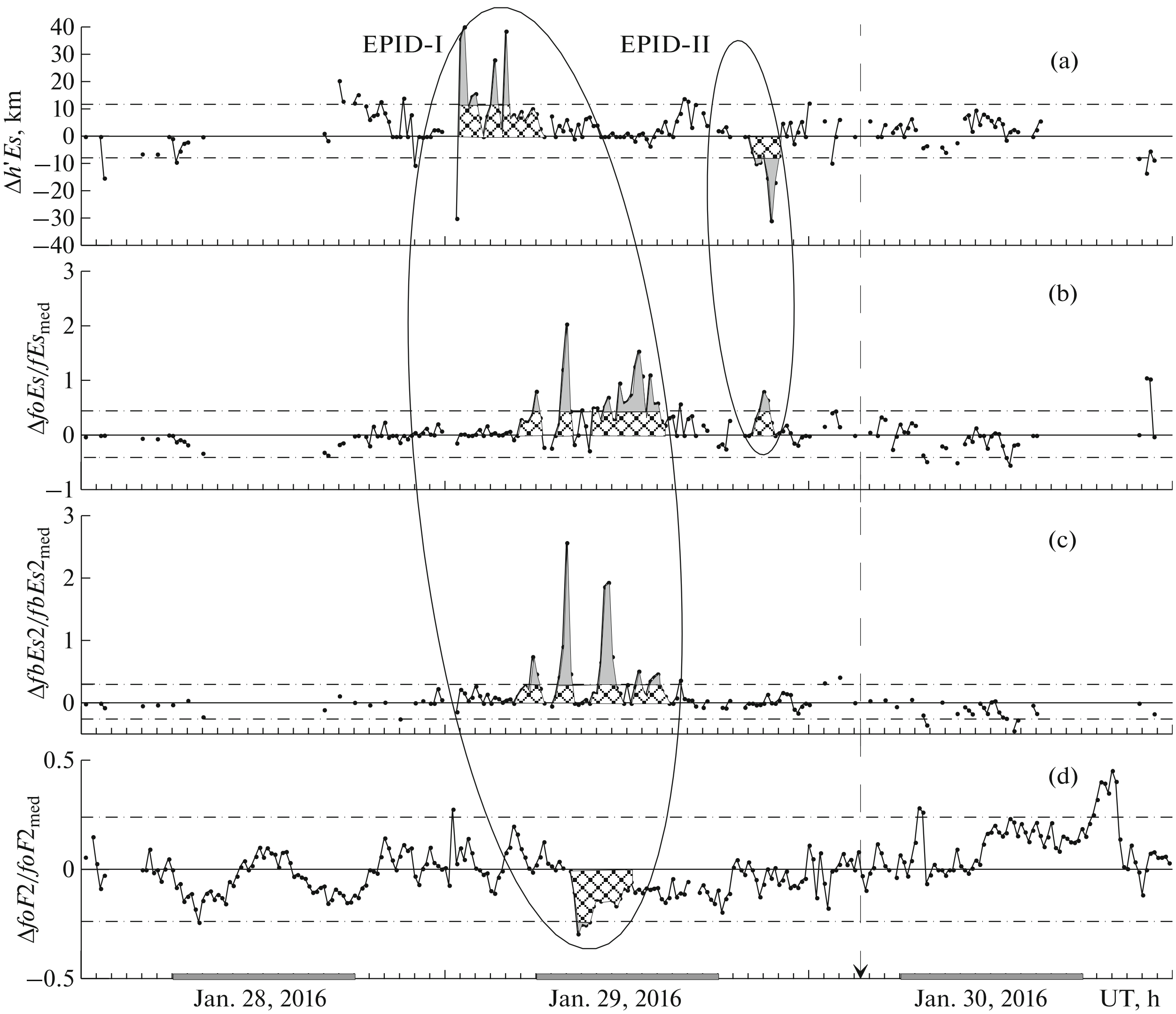

Fig. 1. Temporal variations in parameters of the *Es* and *F*2 ionospheric layers (UT): (a) $\Delta h'Es$, (b) $\Delta foEs/foEs_{med}$, (c) $\Delta fbEs/fbEs_{med}$, (d) $\Delta foF2/foF2_{med}$. Dashed line with arrow marks the moment of earthquake occurrence; dark rectangles on abscissa axis show intervals from 1800 to 0600 LT. Dot-and-dash lines indicate the bands of $K\pm$ scatter, while the variations beyond them (identified anomalies) are shaded in darker tone. Some of these anomalies within the limits of $K\pm$ scatter are hatched for better visual perception. Anomalies are united into two groups (EPID-I and EPID-II ellipses)..

to 0600 LT. The dot-and-dash lines indicate bands of $K\pm$ scatter, while the variations beyond them (identified anomalies) are shaded in darker tone. Some of these anomalies within the limits of $K\pm$ scatter are hatched for better visual perception. The anomalies are united into two groups (EPID-I and EPID-II ellipses).

In the EPID-I group, anomalies of virtual height $h'Es$ appear ~4 h earlier than in the frequency characteristics of the sporadic *Es* region, whereas an anomaly in the *F*2-region appears another 4 h later. Such a distribution of time delay would be valid one assumes that some of the seismic energy is transferred from the solid earth into the upper atmosphere as a result of the development of a seismic process at the final stage of earthquake preparation (close to the moment of occurrence). It first reaches the altitude of the sporadic *Es* region and only then enters the high *F*2-region (the frequency characteristics of these regions are then changed); however, the pattern may be even more complicated. The seismic energy here is understood as the potential energy of the medium, which accumulates in the form of elastic stresses and is then consumed during an earthquake, mainly by the destruction of the medium material, slip friction, and the generation of seismic waves. Before the main rupture, a small part (as compared to the moment of mainshock) of the already accumulated energy is partially released into the atmosphere, e.g., in the form of heat, infrasound, etc. (Ouzounov and Freund, 2004).

The first anomaly in the EPID-I group appeared in *h'Es* ~26.5 h before the earthquake, while the latest (in *foEs* and *fbEs*) ended ~13 h before it. The total duration of anomalies in the group (from the appearance of the first until the disappearance of the last) is ~13 h. Analysis of the EPID-I group of anomalies shows that the virtual height from which reflections are observed considerably increases, and then (with delays of a few hours) the frequencies *fbEs* and *foEs* (not only *fbEs*) abruptly increase, indicating a well-expressed heterogeneity in the horizontal structure of the region. The horizontal dimensions of particular large "clouds," which have higher electron contents, are a few hundreds of kilometers, while the electron content is inhomogeneous within each cloud (B.N. Gershman, 1974). Thus, denser and more heterogeneous plasma clouds appear within the regular *E* region above the ionospheric sounding station, and it is these clouds that comprise the sporadic *Es* region.

Another point should be also mentioned here. For the EPID-I group of anomalies, an abrupt initial decrease in the height of the *h'Es* region correlates with a simultaneous "surge" in *foF*2 (lower panel); however, since the duration of this disturbance is less than half an hour (the only dot), we cannot formally (according to what we assumed above) consider this surge in *foF*2 to be an anomaly, even though it coincides with an abrupt decrease in *h'E*s.

The EPID-II group manifested only in the sporadic *Es* region almost synchronously (in *h'Es* and *foEs*) ~6.4 h before the earthquake and lasted ~1.5 h. Here, the correlation between the increase in *foEs* and decrease in height of the *h'Es* region indicates that the inhomogeneity of the reflecting layer increases simultaneously with its decrease; note that we cannot unambiguously claim that the density of the region increased, because *fbEs* does not almost change.

Figure 2 presents the correlation field of (Ez; λ_Σ) values for the period of January 28–30, 2016, where the curve of nonlinear regression corresponding to the empirical equation $Ez = 7.07 \times 10^2/\lambda_\Sigma^{0.857}$ is shown (solid line), while the standard error of regression is indicated by the dot-and-dash line. The correlation factor for this curve is $\rho = 0.795$. The squared correlation factor, or determination factor, indicates the fraction of variation in the resulting attribute, which is explained by variation of the factor attribute. Most often, when the determination factor is interpreted, it is expressed as a percent, i.e., $\rho^2 = 0.795^2 \cong 0.632$, and it therefore leads to changes of Ez in 63.2% of cases when λ_Σ changes (63.2% of all points falling within the correlation field are between the upper and lower dot-and-dash lines). The remaining 36.8% of changes in Ez are explained by factors that this one-factor model does not take into account. This "theoretical" model is used below to construct the predicted values of Ez based on λ_Σ and the respective theoretical variations in the near-surface atmospheric electricity parameters in order to compare the calculated values with the measured ones.

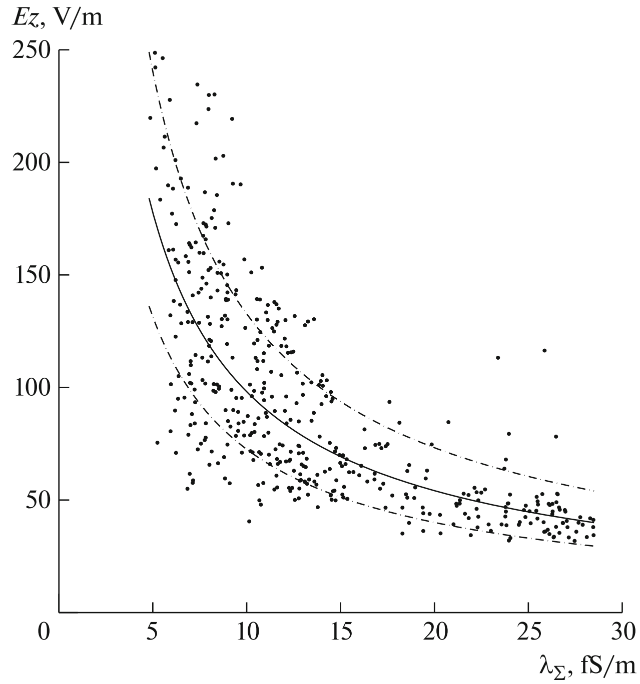

Fig. 2. Correlation field of (Ez; λ_Σ) values for the period of January 28–30, 2016 (dots), the curve of nonlinear regression corresponding to the empirical equation $Ez = 7.07 \times 10^2/\lambda_\Sigma^{0.857}$ (solid line), and the standard error of regression (dot-and-dash line).

As is shown further in Fig. 3, it is these factors (which are not caused by variations in conductivity proper) that probably determine the anomalies in near-surface atmospheric electricity, which in turn can be related to the development of seismic processes. Let us emphasize that variations in the conductivities and values of electrical field Ez at Paratunka Observatory are measured independently from each other.

Figure 3 is analogous to Fig. 1, but shows the respective electrical parameters of the near-surface atmosphere (see section 2). The dashed lines in panels (b) and (c) show variations of the same parameters in accordance with the theoretical model (see Fig. 2). For a higher degree of reliability of anomaly identification, all curves in this figure are smoothed by a 7-point moving window that corresponds to hourly averaging. This smoothing was not applied to the ionospheric data, because these values are often absent in the respective point of diurnal count, especially for the sporadic *Es* layer, whereas data on the electrical characteristics of the near-surface atmosphere for the same moments of time are always available at all points of count. As is clearly seen in Fig. 3, the theoretical curves of relative variations in field and current values

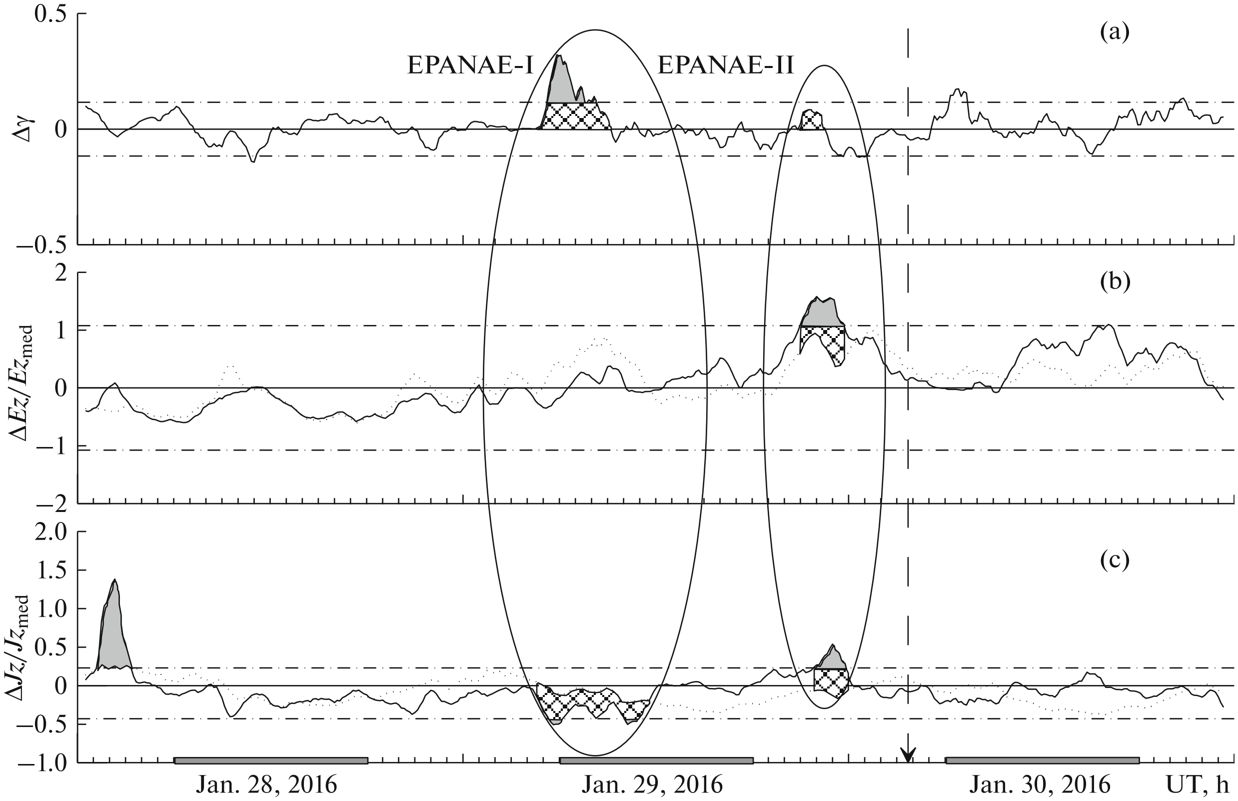

Fig. 3. Same as Fig. 1 for electrical characteristics of the near-surface atmosphere: (a) $\Delta\gamma$, (b) $\Delta Ez/Ez_{\text{med}}$, (c) $\Delta Jz/Jz_{\text{med}}$. Two groups of anomalies are distinguished (EPANAE-I and EPANAE-II ellipses) and also the anomaly of $\Delta Jz/Jz_{\text{med}}$ at the beginning of the day of January 28, 2016. Dashed lines in panels (b) and (c) show variations in these parameters in accord with the theoretical model of dependence $Ez = Ez(\lambda_{\Sigma})$ (see Fig. 2).

are always within the limits of the respective scatter bands.

The anomalies in this figure are also united into two groups (EPANAE-I and EPANAE-II ellipses); a significant relative anomaly of $\Delta Jz/Jz_{\text{med}}$ in the beginning of the day of January 28, 2016 is also indicated.

In the EPANAE-I group, the beginning of positive increments of an augment in the unipolarity factor $\Delta\gamma$ coincides with that of the negative relative increment in vertical current $\Delta Jz/Jz_{\text{med}}$, whereas anomalies of relative changes in vertical component of QAEF Ez are not observed. In terms of time, the EPANAE-I approximately corresponds to the EPID-I group in Fig. 1.

In the EPANAE-II group, the development of a positive relative increment in vertical current $\Delta Jz/Jz_{\text{med}}$ delays relative to the same relative increment of QAEF $\Delta Ez/Ez_{\text{med}}$ by approximately an hour, and the positive absolute increment of unipolarity factor $\Delta\gamma$ approaches the upper boundary of its scatter band in this time. On the time axis, EPANAE-II corresponds to the EPID-II ellipse in Fig. 1.

One particular identified anomaly is a $\Delta Jz/Jz_{\text{med}}$ that existed from 0100 to 0300 UT on January 28, 2016; it was not accompanied by anomalies in other electrical parameters of the near-surface air; however, at ~0130 UT, a negative surge of an increment in virtual height $\Delta h'Es$ was recorded (see Fig. 1). Unfortunately, the ionospheric data on the Es region are too fragmentary for a further time interval (in the vicinity of this time). We can only note that this surge in the increment of virtual height $\Delta h'Es$ in the ionosphere occurred slightly later than the disturbance in near-surface electricity, when the anomaly of $\Delta Jz/Jz_{\text{med}}$ had already developed.

A more detailed comparison of Figs. 1 and 3 via an adjustment of their time axes shows the following. Anomalies in the EPID-II group appear almost synchronously with the onset of the anomaly in QAEP $\Delta Ez/Ez_{\text{med}}$, with an insignificant delay. In the EPID-I group, the pattern is slightly more complicated. Anomalous variations in frequency parameters of the ionosphere, which are closely related to the structure of the sporadic Es layer, also begin with a delay (which is insignificant in the cases of $\Delta foEs/foEs_{\text{med}}$ and $\Delta fbEs/fbEs_{\text{med}}$ and about 4 h in the case of $\Delta foF2/foF2_{\text{med}}$) after the start of anomalies in the EPANAE-I group ($\Delta Jz/Jz_{\text{med}}$ and $\Delta\gamma$ values). However, the height-related characteristics of this $\Delta h'Es$ layer began its anomalous varia-

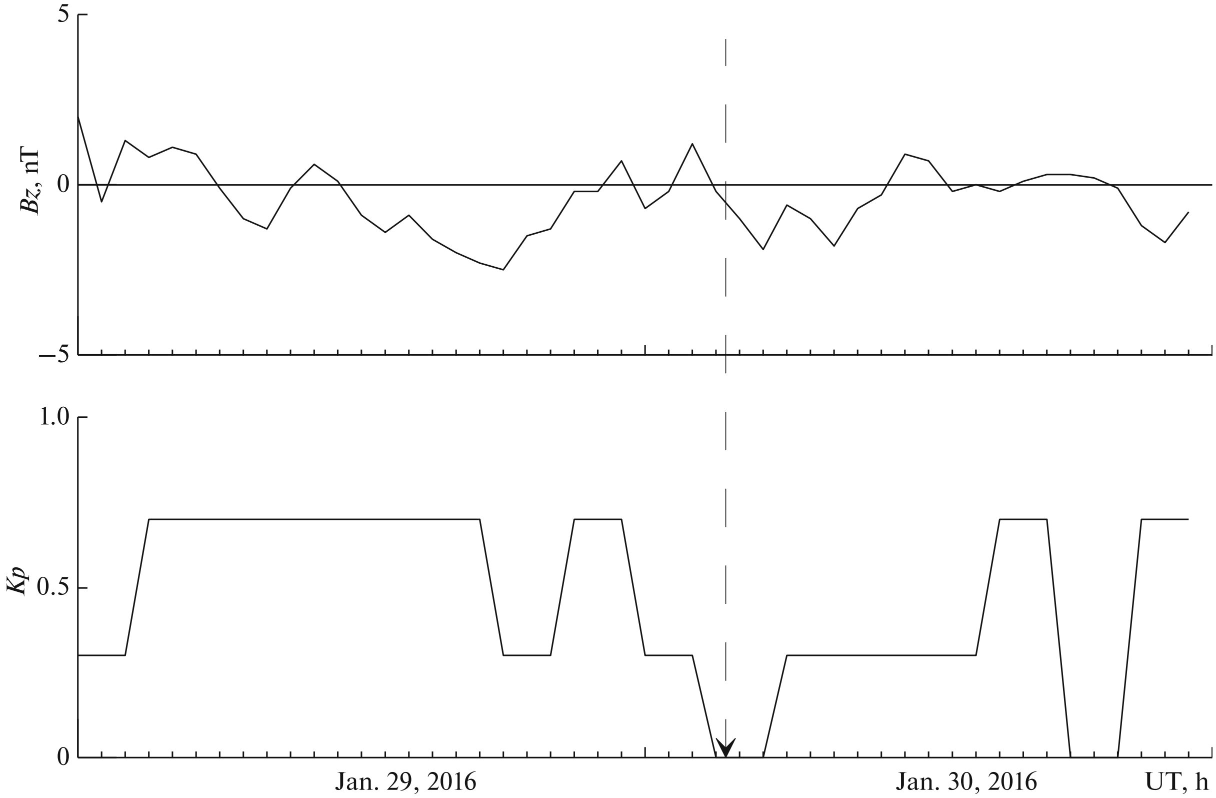

Fig. 4. Temporal variation in *Bz*-component of IMF (upper panel) and *Kp*-index (lower panel) on January 29–30, 2016. Dashed line with arrow marks the moment of earthquake occurrence.

tion about 3 h earlier than the $\Delta Jz/Jz_{\text{med}}$ values became anomalously low (still were negative). Nevertheless, it is seen in Fig. 3 that the $\Delta Jz/Jz_{\text{med}}$ value is not only negative during these 3 h but also passes significantly below the theoretical curve for $\Delta Jz/Jz_{\text{med}}$; i.e., although the $\Delta Jz/Jz_{\text{med}}$ disturbancedoes not cross the lower boundary of its scatter band, the height of the *Es* ionospheric region grows before essential structural changes start in it, which, of course, requires some time.

A comparison of Figs. 1 and 3 demonstrates good agreement between anomalies of the EPID-I and EPANAE-I groups, as well as between the EPID-II and EPANAE-II groups; it also shows the generally earlier development of anomalies in near-surface electricity as compared to the development of ionospheric anomalies. This observed coincidence of temporal variations in ionospheric anomalies and anomalies in near-surface atmosphere before the earthquake of January 30, 2016, supports the hypothesis that these anomalies are related to the process of earthquake preparation and thus are ionospheric earthquake precursors (IEPs) and electrical earthquake precursors (EEPs) for this seismic event, respectively.

Here we should note that the EPID-I and EPID-II groups of anomalies identified in the ionosphere were observed on a very quiet geomagnetic background. To illustrate this, Fig. 4 presents temporal variations in the *Bz*-component of interplanetary magnetic field (IMP) and *Kp*-index on January 29–30, 2016, as constructed based on the data from OMNIWeb (http://omniweb.gsfc.nasa.gov/form/dx1.html; the dashed line with arrow marks the moment of earthquake occurrence). It is clearly seen that the value of *Kp*-index for all hours of the day did not exceed 1_-, and the value of *Bz*-component of the IMF did not fall below −2.5 nT. In addition, the very fact that the well-expressed sporadic *Es* layer appeared is indirect evidence of a quiet time of the geomagnetic field, because a negative correlation between the probability of the appearance of *Es* region and magnetic activity is observed in the zone of geomagnetic latitudes 30°–50° (Chavdarov et al., 1975), the while geomagnetic latitude of the Paratunka Observatory is ~46°.

Generally speaking, analysis of ionospheric disturbances always requires special and thorough testing for their possible relationship with geomagnetic disturbances. Thus, in the work by Astafyeva and Heki (2011) in which seismoionospheric anomalies were studied from measurements of integrated characteristics of the total electron content (TEC) in the ionosphere, it was shown that, in certain conditions, negative excursions of the *Bz*-component of the IMF as large as –5...–7 nT are sufficient to exceed the median background TEC of up to 20–30%.

However, even if we apply these results to our studied case without taking into consideration the fact that our study deals with local ionospheric parameters, we can see that, on the one hand, the minimal "cutoff" level we obtained to determine an anomaly in frequency parameters was ~23% for $\Delta foF2/foF2_{\rm med}$ (it is slightly higher for other frequency parameters); on the other hand, interpolating the results from Astafyeva and Heki (2011) to the observed limit negative value of the *Bz*-component of the IMF from our work (–2.5 nT), we obtain the maximal absolute value of possible deviation from the background, ~7.5%, that can be connected with this negative excursion of *Bz*-component of the IMF.

5. CONCLUSIONS

A comparative analysis of the data from vertical ionospheric sounding (15-min sampling frequency) and measurements of the vertical *Ez* component of near-surface quasistatic atmospheric electrical field (with the respective values of electrical conductivity of near-surface air, λ^+ and λ^-), recorded at the Paratunka complex geophysical observatory for the period from January 28 to January 30, 2016, has been conducted. The goal was to reveal possible anomalies preceding an earthquake with $M = 7.2$ that occurred on January 30, 2016, at 0325 UT at an epicentral distance of 117 km from the observatory.

As was revealed, the identified groups of earthquake-preceding ionospheric disturbances (EPID-I and EPID-II) demonstrate good temporal correlation with the anomalies in near-surface atmospheric electricity that preceded the earthquake (EPANAE-I and EPANAE-II). Taking into account earlier studies on the search for ionospheric precursors of earthquakes in the Kamchatka region (Korsunova and Hegai, 2013), we can think with quite a high degree of confidence that the identified ionospheric anomalies were IEPs and that the respective anomalies in near-surface atmospheric electricity were EEPs of the mentioned seismic event.

ACKNOWLEDGMENTS

We thank Z.F. Dumbrava for her assistance with this work and also NASA's Goddard Space Flight Center, United States, for granting the data on the *Kp* planetary index of geomagnetic activity and *Bz*-component of the IMF.

REFERENCES

Aprodov, V.A., *Zony zemletryasenii* (Earthquake Zones), Moscow: Mysl', 2000.

Astafyeva, E.I. and Heki, K., Vertical TEC over seismically active region during low solar activity, *J. Atmos. Sol.-Terr. Phys.*, 2011, vol. 73, no. 13, pp. 1643–1652. doi 10.1016/j.jastp.2011.02.020

Chavdarov, S.S., Chasovitin, Yu.K., Chernysheva, S.P., and Sheftel', V.M., *Sredneshirotnyi sporadicheskii sloi E ionosfery* (Midlatitude Sporadic E Layer of the Ionosphere), Moscow: Nauka, 1975.

Chen, Y.-I., Liu, J.-Y., Tsai, Y.-B., and Chen, C.-S., Statistical tests for pre-earthquake ionospheric anomaly, *Terr. Atmos. Ocean. Sci. J.*, 2004, vol. 15, no. 3, pp. 385–396.

Elektromagnitnye predvestniki zemletryasenii (Electromagnetic Earthquake Precursors), Sadovskii, M.A., Ed., Moscow: Nauka, 1982.

Encyclopedia of Statistical Sciences, Klotz, S. and Johnson, N.L., Eds., New Jersey: John Wiley, Hoboken, 1983.

Freund, F.T., Takeuchi, A., and Lau, B.W.S., Electric currents streaming out of stressed igneous rocs—a step towards understanding pre-earthquake low frequency EM emissions, *Phys. Chem. Earth. Parts A/B/C*, 2006, vol. 31, nos. 4–9, pp. 389–396.

Gershman, B.N., *Dinamika ionosfernoi plazmy* (Ionospheric Plasma Dynamics), Moscow: Nauka, 1974.

http://wdc.kugi.kyoto-u.ac.jp/index.html.

Korsunova, L.P. and Hegai, V.V., Analysis of seismoionospheric disturbances at the chain of Japanese stations for vertical sounding of the ionosphere, *Geomagn. Aeron. (Engl. Transl.)*, 2008, vol. 48, no. 3, pp. 392–399.

Korsunova, L.P. and Hegai, V.V., On the efficiency of the method of search for ionospheric earthquake precursors from the sporadic *E* and regular *F*2 layer parameters, in *Sbornik dokladov VI Mezhdunarodnoi konferentsii "Solnechno–zemnye svyazi i fizika predvestnikov zemletryasenii", Paratunka, Kamchatskii krai, 9–13 sentyabrya 2013 g.* (Proceedings of the VI International Conference "Solar–Terrestrial Relations and Physics of Earthquake Precursors," Paratunka, Kamchatka, September 9–13, 2013), Shevtsov, B.M., Ed., Petropavlovsk-Kamchatskii: IKIR DVO RAN, 2013, pp. 412–417.

Korsunova, L.P. and Hegai, V.V., Ionospheric precursors of crustal earthquakes in the northwestern part of the Asia-Pacific seismic belt, *Open Trans. Geosci. (GEOS)*, 2014, vol. 1, no. 1, pp. 25–33.

Korsunova, L.P. and Hegai, V.V., Effectiveness criteria for methods of identifying ionospheric earthquake precursors by parameters of a sporadic e layer and regular *F*2 layer, *J. Astron. Space Sci.*, 2015, vol. 32, no. 2, pp. 137–140.

Liperovskii, V.A., Pokhotelov, O.A., and Shalimov, S.L., *Ionosfernye predvestniki zemletryasenii* (Ionospheric Earthquake Precursors), Moscow: Nauka, 1992.

Liu, J.Y., Chen, Y.I., Chuo, Y.J., and Chen, C.S., A statistical investigation of pre-earthquake ionospheric anomaly, *J. Geophys. Res.*, 2006, vol. 111, A05304. doi 10.1029/2005JA011333

Mikhailov, Yu.M., Mikhailova, G.A., Kapustina, O.V., Buzevich, A.V., and Smirnov, S.E., Specific features of atmospheric noise superimposed on variations in the quasistatic electric field in the Kamchatka near-Earth atmosphere, *Geomagn. Aeron. (Engl. Transl.)*, 2005, vol. 45, no. 5, pp. 649–664.

Nestorov, G.T., A possible ionospheric presage of the Vrancha earthquake of March 4, 1977, *C. R. Acad. Bulg. Sci.*, 1979, vol. 32, no. 4, pp. 443–446.

Ouzounov, D. and Freund, F.T., Mid-infrared emission prior to strong earthquakes analyzed by remote sensing data, *Adv. Space Res.*, 2004, vol. 33, no. 3, pp. 268–273.

Prölss, G.W., Ionospheric *F*-region storms, in *Handbook of Atmospheric Electrodynamics*, Volland, H., Ed., Boca Raton, Florida, CRC, 1995, vol. 2, ch. 8, pp. 195–248.

Rishbeth, H., *F*-region storms and thermospheric dynamics, *J. Geomagn. Geoelectr.*, 1991, vol. 43, suppl. 1, pp. 513–524.

Rulenko, O.P., Operativnye predvestniki zemletryasenii v elektrichestve prizemnoi atmosfery, *Vulkanol. Seismol.*, 2000, no. 4, pp. 57–68.

Rulenko, O.P., New technique for revealing and studying earthquake precursors in electricity of the surface atmosphere, *Vestn. Kamchatskoi Reg. Assots. Uchebno-Nauchnyi Tsentr, Nauki Zemle*, 2008, vol. 2, no. 12, pp. 42–47.

Sidorin, A.Ya., *Predvestniki zemletryasenii* (Earthquake Precursors), Moscow: Nauka, 1992.

St-Laurent, F., Derr, J.S., and Freund, F.T., Earthquake lights and the stress-activation of positive hole charge carriers in rocks, *Phys. Chem. Earth. Parts A/B/C*, 2006, vol. 31, nos. 4–9, pp. 305–312.

Translated by N. Astafiev